

Chemical Synthesis of Face-centered-tetragonal FePt Film Using Sol–Gel Method

Hailin Su,^{*1,2} Nujiang Tang,² Ruilong Wang,² Bai Nie,² Shaolong Tang,^{*2} Liya Lv,² and Youwei Du²

¹*School of Material Science and Engineering, Hefei University of Technology, Hefei 210009, P. R. China*

²*National Laboratory of Solid State Microstructure and Department of Physics, Nanjing University, Nanjing 210093, P. R. China*

(Received September 22, 2006; CL-061105; E-mail: tangsl@nju.edu.cn)

A simple sol–gel spin-coating technique was developed to prepare FePt films. The calcining temperature was found to have great influences on the film's crystalline structure and magnetic properties. For this method, pure face-centered-tetragonal FePt film was finally obtained by calcining at 370 °C and subsequently reducing at 470 °C.

The ordered face-centered-tetragonal (fct) FePt has large magnetocrystalline anisotropy constant, moderate magnetization, and excellent chemical and thermal stabilities. Due to the potential applications in high-density recording media and the magnetic component of the microelectromechanical systems, films based on it have attracted much attention.^{1,2} Generally, FePt films are prepared by vacuum techniques such as magnetron sputtering,³ molecular beam epitaxy,⁴ and pulsed laser deposition.⁵ Because these techniques are complicated and of high cost, chemically synthetic methods, such as electrochemical deposition⁶ and solution phase chemical synthesis,⁷ are developed and adopted more frequently in recent years owing to their advantages of inexpensive apparatus and facile operation. However, as a powerful chemical preparation technique, the sol–gel method has not been used to fabricate FePt films yet. In this paper, we explore the possibility of using a sol–gel spin-coating technique to fabricate FePt films and investigate the influences of the heating temperature on the film's crystalline structure and magnetic properties.

The thin FePt films with thickness of about 30 nm, measured by an α -step, were prepared by a sol–gel process and spin-coating technique. To prepare the sol solution, 100 mL ethanol solution consisting of 0.01 mol $\text{FeCl}_2 \cdot 4\text{H}_2\text{O}$, 0.01 mol $\text{H}_2\text{PtCl}_6 \cdot 6\text{H}_2\text{O}$, and 0.06 mol citric acid monohydrate was firstly stirred at 60 °C for 6 h. Then, 0.1 mL *N,N*-dimethylformamide was added into the solution as a drying chemical control agent, and the mixed solution was stirred at 60 °C again for 0.5 h. After these operations, the sol solution was spin-coated onto the thermally oxidized silicon substrates at 3000 rpm for 30 s and dried in air at 100 °C to prepare the precursor film. The dried precursor films were then calcined at varying temperatures T_{cal} ranging from 320 to 470 °C in oxygen ambient for 5 min and subsequently reduced at the temperature T_{red} of 470 °C in flowing hydrogen for 35 min. Induction-coupled plasma spectrometer analyses demonstrate that the Fe:Pt atomic ratio in the formed final films is consistent with that in the initial sol solution, namely 1:1.

X-ray diffraction (XRD, D/Max-RA with $\text{Cu K}\alpha$ radiation) was used to characterize the crystalline structure of the films. Figure 1a shows the XRD patterns of the films calcined at different temperatures T_{cal} (320–470 °C). In the pattern of the film calcined at 320 °C, we cannot find any diffraction peaks relating to the oxides of Fe but two Pt_3O_4 peaks. This may be

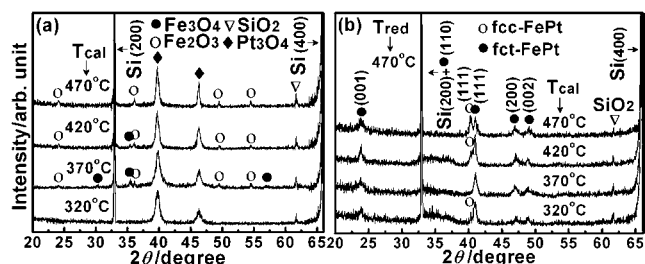


Figure 1. XRD patterns of (a) the calcined films and (b) the reduced final films. The calcining temperatures T_{cal} are 320, 370, 420, and 470 °C and the reducing temperature T_{red} is 470 °C.

due to the incomplete thermooxidative decomposition of the organometallic precursor according to the thermogravimetric differential thermal analysis.⁸ When T_{cal} increases to 370 °C, the diffraction peaks corresponding to Fe_3O_4 and Fe_2O_3 appear in the pattern of the film. With further increasing T_{cal} , some Fe_3O_4 peaks disappear while all the Fe_2O_3 peaks still remain in the pattern. When T_{cal} increases to 470 °C, the Fe_3O_4 diffraction peaks vanish completely, and the film only consists of Fe_2O_3 and Pt_3O_4 . It is clear that both the components and their contents are different for the films calcined at different T_{cal} . From Figure 1a, it can also be found that the Pt_3O_4 peaks become narrower with increasing T_{cal} , which suggests that high T_{cal} favors the growth of crystalline grains. Figure 1b shows the XRD patterns of the final reduced films. It is clear that after the reduction, the final film calcined at 320 °C comprises fct FePt and a trace amount of fcc FePt. An increase of T_{cal} to 370 °C results in the formation of pure fct FePt final film. With further increasing T_{cal} to 420 °C or above, the fcc FePt appears in the final films again, and its content increases with increasing T_{cal} . This implies that the more Fe_2O_3 and the larger crystalline grains may retard the formation of fcc FePt more and hence the fcc–fct ordering transformation is inhibited. Comparing these four patterns, we can find that all the final films contain fct FePt, which indicates that the fcc–fct ordering transformation temperature can be lowered to 470 °C for our method. It is believed that atomically ordered fct FePt fractions, which firstly nucleate at the sites of the lattice defects within some fcc FePt regions, induce the transformation at this relatively low temperature.^{9–11}

Based on these XRD analyses, the possible mechanism of our method can be concluded as follows. Firstly, the sol–gel process yields the organometallic precursor. Then, the precursor thermooxidatively decomposes into the iron oxides and the platinum oxide after calcining above a certain temperature for a sufficient time. But if the calcining temperature T_{cal} is low, large amounts of organometallic precursor will decompose incompletely. During the forefront of the reduction process, these resid-

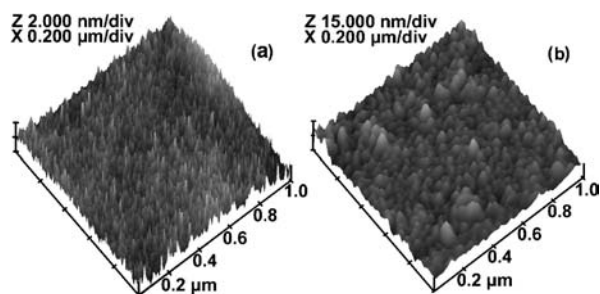


Figure 2. AFM images of (a) the oxide film ($T_{\text{cal}} = 370^{\circ}\text{C}$) and (b) the fct FePt film ($T_{\text{cal}} = 370^{\circ}\text{C}$, $T_{\text{red}} = 470^{\circ}\text{C}$).

ual organometallic substances are directly pyrolyzed and then form fcc FePt, while those formed oxides are firstly reduced into Fe and Pt and then form fcc FePt through the atomic diffusion between Fe and Pt. With further extending the reducing time or increasing the reducing temperature, the disordered fcc FePt transformed into the ordered fct FePt gradually. According to this mechanism, we can deduce that for films calcined below and above 370°C , increasing the reducing temperature or extending the reducing time may be an appropriate means to achieve the complete fcc–fct transformation. Further investigations to evidence it are currently in progress.

The morphologies of the films were investigated by an atomic force micrograph (AFM, Digital Instruments Nanoscope IIIa). The AFM surface images of the oxide film ($T_{\text{cal}} = 370^{\circ}\text{C}$) and the fct FePt film ($T_{\text{cal}} = 370^{\circ}\text{C}$, $T_{\text{red}} = 470^{\circ}\text{C}$) are shown in Figure 2. It can be seen that the oxide film is fairly flat. After the reduction, the film surface roughness deteriorates apparently. The root-mean-squared roughnesses for the oxide film and the fct FePt film are 0.438 and 2.542 nm, respectively.

The in-plane magnetic properties of the reduced films were measured by a superconducting quantum interference device magnetometer (Quantum Design, MPMSXL-7) at room temperature. Figure 3 shows the maximum magnetizations M_{4T} , coercivities H_c , and squarenesses M_r/M_{4T} as functions of the calcining temperature T_{cal} . Here, it should be noted that the magnetic data shown in Figure 3 are the ones after subtracting the linear diamagnetic background of the Si/SiO₂ substrate and that M_{4T} represents the magnetization measured at 40 kOe. It can be seen that with increasing T_{cal} , H_c and M_r/M_{4T} firstly increase and then decrease while the variation of M_{4T} shows an opposite tendency. This result can be attributed to the different film components caused by different T_{cal} . According to the XRD analyses, the final film whose T_{cal} is 370°C only consists of single fct FePt phase, while those calcined above or below 370°C are actually the mixture of fcc FePt and fct FePt. Because the fcc phase is magnetically soft and has a saturation magnetization higher than that of the fct phase, the decrease of fcc FePt in the film may undoubtedly result in the deterioration of M_{4T} and the improvement of H_c and M_r/M_{4T} . From Figure 3, we can see that the pure fct FePt film ($T_{\text{cal}} = 370^{\circ}\text{C}$, $T_{\text{red}} = 470^{\circ}\text{C}$) possesses the relatively lowest M_{4T} ($0.902\text{ k-emu-cc}^{-1}$) but highest H_c

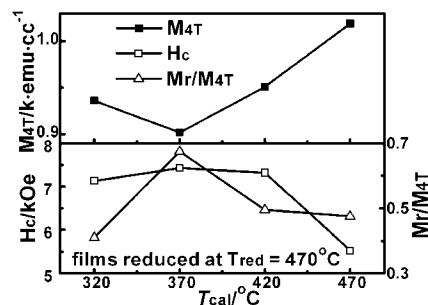


Figure 3. In-plane maximum magnetizations M_{4T} , coercivities H_c and squarenesses M_r/M_{4T} of films reduced at 470°C as functions of the calcining temperature T_{cal} .

(7.43 kOe) and M_r/M_{4T} (0.675). This hard magnetic performance is fairly good compared to those of some films annealed at about 500°C .^{3,4,6} But H_c is not as high as those of films annealed at higher temperatures,^{5–7} indicating a moderate ordering degree for the fct FePt film prepared by our method.

In conclusion, a simple sol–gel spin-coating technique was successfully developed to prepare FePt films. The components and the magnetic properties of the films were found to have great dependences on the calcining temperature. Only the film calcined at 370°C and subsequently reduced at 470°C comprise single fct FePt phase. For this pure fct FePt film, its maximum magnetization M_{4T} , coercivity H_c , and squareness M_r/M_{4T} are $0.902\text{ k-emu-cc}^{-1}$, 7.43 kOe , and 0.675 , respectively.

This work was supported by the National Key Project of Fundamental Research of China (No. 2005CB623605).

References and Notes

- 1 T. Mahalingam, J. P. Chu, J. H. Chen, S. F. Wang, K. Inoue, *J. Phys.: Condens. Matter* **2003**, *15*, 2561.
- 2 K. Barmak, J. Kim, L. H. Lewis, K. R. Coffey, M. F. Toney, A. J. Kellock, J. U. Thiele, *J. Appl. Phys.* **2004**, *95*, 7501.
- 3 C. M. Kuo, P. C. Kuo, H. C. Wu, Y. D. Yao, C. H. Lin, *J. Appl. Phys.* **1999**, *85*, 4886.
- 4 J. P. Attané, Y. Samson, A. Marty, D. Halley, C. Beigné, *Appl. Phys. Lett.* **2001**, *79*, 794.
- 5 M. Weisheit, L. Schultz, S. Fähler, *J. Appl. Phys.* **2004**, *95*, 7489.
- 6 E. B. Svedberg, J. J. Mallett, S. Sayan, A. J. Shapiro, W. F. Egelhoff, T. Moffat, *Appl. Phys. Lett.* **2004**, *85*, 1353.
- 7 F. Iskandar, T. Iwaki, T. Toda, K. Okuyama, *Nano Lett.* **2005**, *5*, 1525.
- 8 Supporting Information is available electronically on the CSJ-Journal Web site, <http://www.csj.jp/journals/chem-lett/index.html>.
- 9 M. Molotskii, V. Fleurov, *Phys. Rev. B* **2001**, *63*, 132102.
- 10 S. R. Lee, S. Yang, Y. K. Kim, J. G. Na, *J. Appl. Phys.* **2002**, *91*, 6857.
- 11 B. Jeyadevan, A. Hobo, K. Urakawa, C. N. Chinnasamy, K. Shinoda, K. Tohji, *J. Appl. Phys.* **2003**, *93*, 7574.